Pathogenesis of retinitis pigmentosa associated with apoptosis-inducing mutations in carbonic anhydrase IV

Rupak Datta, Abdul Waheed, Giuseppe Bonapace, Gul N. Shah, and William S. Sly[1]

Edward A. Doisy Department of Biochemistry and Molecular Biology, Saint Louis University School of Medicine, St. Louis, MO 63104

Contributed by William S. Sly, December 23, 2008 (sent for review November 25, 2008)

Missense mutations in the carbonic anhydrase IV (CA IV) gene have been identified in patients with an autosomal dominant form of retinitis pigmentosa (RP17). We used two transient expression systems to investigate the molecular mechanism by which the newly identified CA IV mutations, R69H and R219S, contribute to retinal pathogenesis. Although the R219S mutation drastically reduced the activity of the enzyme, the R69H mutation had a minimal effect, suggesting that loss of CA activity is not the molecular basis for their pathogenesis. Defective processing was apparent for both mutant proteins. Cell surface-labeling techniques showed that the R69H and R219S mutations both impaired the trafficking of CA IV to the cell surface, resulting in their abnormal intracellular retention. Expression of both CA IV mutants induced elevated levels of the endoplasmic reticulum (ER) stress markers, BiP and CHOP, and led to cell death by apoptosis. They also had a dominant-negative effect on the secretory function of the ER. These properties are similar to those of R14W CA IV, the signal sequence variant found in the original patients with RP17. These findings suggest that toxic gain of function involving ER stress-induced apoptosis is the common mechanism for pathogenesis of this autosomal-dominant disease. Apoptosis induced by the CA IV mutants could be prevented, at least partially, by treating the cells with dorzolamide, a CA inhibitor. Thus, the use of a CA inhibitor as a chemical chaperone to reduce ER stress may delay or prevent the onset of blindness in RP17.

autosomal dominant | chemical chaperone | ER stress | missense mutation | Na+/bicarbonate co-transporter 1

Retinitis pigmentosa (RP) is a group of progressive eye diseases characterized by the deaths of retinal photoreceptors. Patients suffer from night blindness, gradual constriction of visual fields, and eventual loss of central vision (1). Increasing evidence points to a causative role for mutations in the carbonic anhydrase IV (CA IV) gene in pathogenesis of RP17, an autosomal dominant form of RP (2–4).

Three different missense mutations in the coding region of CA IV have been discovered. The first was a signal sequence mutation, changing Arg^{14} to Trp (R14W) (2). The other 2 mutations change amino acids in the mature portion of the protein, replacing Arg^{69} and Arg^{219} with His and Ser, respectively (R69H and R219S) (3, 4). RP associated with the R14W and R219S mutations is inherited in an autosomal-dominant fashion (2, 3). The R69H mutation was found in a sporadic case of RP (4). Because CA IV is not expressed in the retina (5), explaining the pathogenesis of RP17 presented a challenge. Understanding the pathogenesis is essential to design mechanism-based therapies for this disease for which no effective treatment is currently available.

CA IV is synthesized in the endoplasmic reticulum (ER) as a 312-amino acid precursor (6). After several post-translational modifications, the mature form is expressed as a glycosylphosphatidylinositol (GPI)-anchored protein in the plasma membranes of epithelial and endothelial cells of different organs, including the choriocapillaris of the eye (5, 7). We previously showed that the R14W mutation in the signal sequence of CA IV reduced the steady-state level of the protein by nearly 30% in transfected COS-7 cells through a combination of decreased synthesis and accelerated turnover (2). Expression of the mutant protein also induced ER stress and apoptotic cell death. Because CA IV is highly expressed in the choriocapillaris of the eye but not in the retina (5), we proposed that ER stress-induced apoptosis of endothelial cells in the choriocapillaris might cause secondary damage in the overlying retina that eventually leads to RP (2). Subsequent studies provided evidence that the toxic gain of function of the R14W mutation can be reversed by several well-characterized CA inhibitors that act as pharmacological chaperones, thereby providing a strategy for treating the disease (8).

However, an alternate hypothesis was proposed to explain the retinal pathogenesis of R14W and 2 other CA IV mutants (R69H and R219S) (3, 4). According to this hypothesis, a CA IV-Na^+/bicarbonate co-transporter 1 (NBC1) complex (metabolon) in endothelial cells of the choriocapillaris is involved in maintaining the pH balance of the retina. Loss of function of 1 CA IV allele due to these missense mutations is proposed to negatively impact retinal pH homeostasis and lead to loss of retinal integrity. Moreover, proponents of this hypothesis argue that long-term use of CA inhibitors should also create a functional deficiency of CA IV and disrupt retinal integrity, even for those without CA IV mutations. However, this hypothesis does not adequately explain how loss of only 1 functional CA IV allele can cause retinal degeneration and lead to a dominant disease. Furthermore, lack of any retinal abnormality in the CA IV-knockout (KO) mice indicated that even total loss of CA IV function did not cause retinal disease in the mouse (9).

In this report, we analyzed the 2 additional CA IV mutations (R69H and R219S) that others reported in RP17 patients (3, 4) and attempt to reconcile the 2 hypotheses to explain the mechanism by which these mutations lead to RP. Results presented here show that both new mutations also lead to protein misfolding and impaired trafficking of the CA IV protein and produce ER stress that leads to apoptosis. These findings support a toxic gain of function as a molecular basis for their pathogenicity. Furthermore, as was true for R14W CA IV, cell death caused by expression of these mutants can be reduced by treating the cells with a commonly used CA inhibitor, dorzolamide, suggesting a general strategy for the prevention and/or treatment of RP17.

Results

Effect of R69H and R219S Mutations on CA IV Expression in Transfected COS-7 Cells. To elucidate the mechanism underlying the retinal pathogenicity of the R69H and R219S CA IV mutants, we expressed them in COS-7 cells and compared their activity to

Author contributions: R.D., A.W., G.B., G.N.S., and W.S.S. designed research; R.D., G.B., and G.N.S. performed research; A.W. contributed new reagents/analytic tools; R.D., A.W., and W.S.S. analyzed data; and R.D., A.W., and W.S.S. wrote the paper.

The authors declare no conflict of interest.

[1]To whom correspondence should be addressed. E-mail: slyws@slu.edu.

Table 1. Comparison of CA IV activity in lysates from transfected COS-7 cells expressing WT or mutant CA IV

cDNA	CA activity*, units/mg	Percentage
CA IV WT	2.4 ± 0.12	100
CA IV R69H	2.08 ± 0.09	86.6
CA IV R219S	0.18 ± 0.05	7.5

*Average of three separate transfection experiments with two independent measurements per transfection.

that of the wild-type counterpart. Data in Table 1 show that the R219S mutation resulted in a drastic loss of CA IV activity (>90%), whereas reduction in activity from the R69H mutation was quite mild (≈14%). These results are in agreement with earlier reports where the enzymes were expressed in HEK-293 cells (3, 4). On western blots, we observed a 13% and 35% reduction in the CA IV expression level owing to the R69H and R219S mutation, respectively (Fig. 1 *A* and *B*). The loss in activity for the R69H mutation was thus proportional to the reduced level of the protein expressed. However, the R219S substitution nearly abolished the catalytic activity of the CA IV protein expressed, most likely because of its proximity to the active-site cleft (10). The fact that reduction in activity is barely detectable for the R69H mutant argues that loss of CA IV activity itself does not explain the retinal pathology in RP17.

To examine the processing of the enzyme in transfected cells, we used nonreducing SDS/PAGE. With this technique, the slow-migrating, unfolded precursor form of CA IV can be resolved from the faster-migrating, more compact form of the mature protein (11). Cells expressing the R69H or the R219S mutants show a larger fraction of the slow-migrating precursor compared to those expressing wild-type CA IV (Fig. 1*C*). This result suggests that both mutations impair processing.

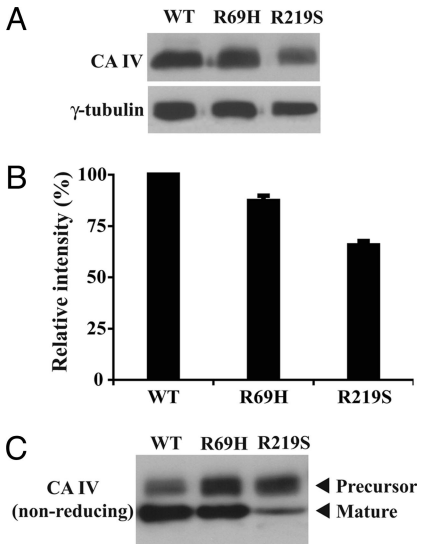

Fig. 1. Western blot analysis in COS-7 cells expressing the wild-type or mutant CA IVs. (*A*) Total protein (12.5 μg) from COS-7 cells transfected with cDNAs expressing wild-type, R69H, or R219S CA IV was subjected to reducing SDS/PAGE and blotted either with CA IV antibody to measure CA IV expression level (*Upper*) or with γ-tubulin antibody to normalize the differences in loading (*Lower*). (*B*) Densitometry analyses of the blots to quantitate relative levels of CA IV expression. (*C*) Total protein (12.5 μg) from each of the transfected cells was resolved under nonreducing conditions and subjected to western blot with CA IV antibody. Arrows indicate positions of the precursor and mature forms of CA IV (11).

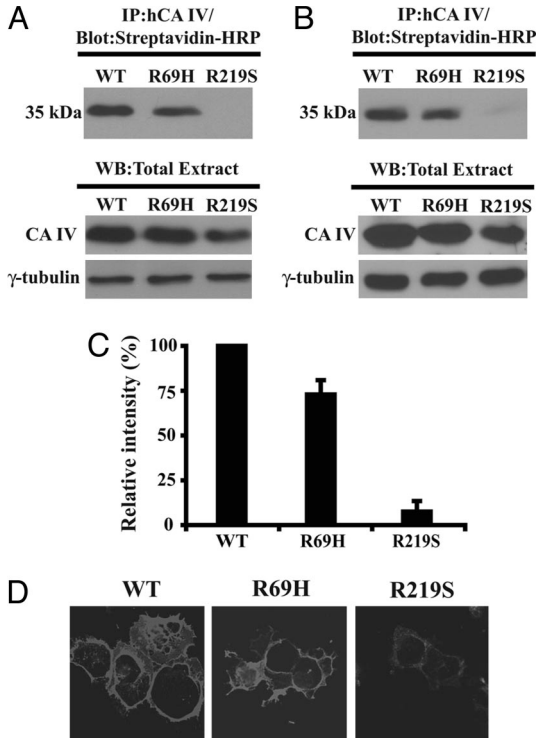

Fig. 2. Effect of R69H and R219S mutations on cell-surface expression of CA IV. (*A*) COS-7 or (*B*) HEK-293 cells expressing either wild-type, R69H, or R219S CA IV were cell-surface biotinylated. Lysates (100 μg total protein) were immunoprecipitated (IP) with CA IV antibody and immunoprecipitates were analyzed on a 10% SDS/PAGE. The blots were probed with streptavidin-peroxidase. Note the position of CA IV (35 kDa) (*Upper*). Parts of the lysate were subjected to western blot (WB) with indicated antibodies (*Lower*). (*C*) Densitometry analysis of the blots to quantitate relative cell-surface expression of CA IV in both the cell types. (*D*) COS-7 cells were transfected with wild-type, R69H, or R219S CA IV, immunostained with CA IV antibody under nonpermeabilized conditions followed by Alexafluor-546-conjugated secondary antibody, and visualized by fluorescence microscopy. Images were converted into gray-scale using Adobe Photoshop CS software (Adobe Systems Incorporated).

Effects of R69H and R219S Mutations in Trafficking of CA IV to the Cell Surface. For this analysis, we performed cell-surface biotinylation on transfected COS-7 cells. After cell lysis, immunoprecipitation with CA IV antibody, and separation of the immunoprecipitates on SDS/PAGE, the cell surface CA IVs were detected by blotting with streptavidin-HRP (Fig. 2*A*, *Upper*). Parts of lysates were subjected to western blot analysis with CA IV antibody to estimate total CA IV expression and with γ-tubulin antibody to confirm uniform loading (Fig. 2*A*, *Lower*). Fig. 2*A* shows that the relative abundance of the R219S mutant on the cell surface was markedly reduced compared with that of the wild-type CA IV. Cell-surface expression for the R69H mutant was also reduced, but to a lesser extent. These data contrast with previous reports that cell surface expression of these mutants was similar to that of the wild-type CA IV in a HEK-293 expression system (3, 4). To explore whether this discrepancy was due to a cell-type difference, we performed cell-surface biotinylation experiments in transfected HEK-293 cells. The results were the same as in transfected COS-7 cells (Fig. 2*B*). Densitometric quantitation of multiple experiments on COS-7 and HEK-293 cells showed an average reduction in CA IV cell surface expression of 30% and 90% owing to the R69H and R219S mutations, respectively (Fig. 2*C*).

We also performed immunocytochemistry in nonpermeabilized cells so as to label only the cell surface-localized CA IV

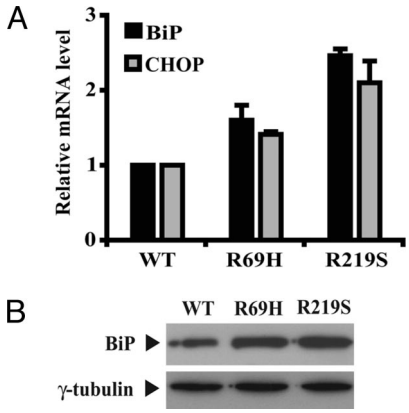

Fig. 3. Status of ER stress markers in cells expressing the wild-type or mutant CA IVs. (*A*) RNA was isolated from HEK-293 cells expressing wild-type, R69H, or R219S CA IV, and relative BiP (black bars) and CHOP (gray bars) mRNA levels were measured by RT-qPCR. Error bars represents SD from triplicate data. (*B*) Western blot analyses in COS-7 cells (12.5 μg total protein) expressing either wild-type, R69H, or R219S CA IV with BiP (*Upper*) and γ-tubulin (*Lower*) antibody.

(Fig. 2*D*). Here, we also observed very little expression of R219S CA IV on the cell surface. Cell surface staining for the R69H mutant was also somewhat reduced compared with wild-type. Thus, both the R69H and R219S mutations disrupt processing and trafficking of CA IV, but to different degrees.

Expression of R69H and R219S CA IV Mutants Induces ER Stress. Abnormal accumulation of unfolded protein in the ER causes ER stress to which the cells respond by initiating a complex signal transduction pathway called the unfolded protein response (12). To test whether accumulation of unprocessed mutant CA IVs induced ER stress, we examined expression of two common ER stress markers, BiP and CHOP, in transfected HEK-293 cells by real-time quantitative PCR (RT-qPCR) (Fig. 3*A*). Cells expressing R69H CA IV had 1.6- and 1.4-fold higher levels of BiP and CHOP mRNA, respectively, relative to those produced by wild-type cDNA. Expression of the R219S variant resulted in stronger up-regulation of the ER stress markers (2.4- and 2.1-fold for BiP and CHOP, respectively). ER stress was also analyzed in transfected COS-7 cells by western blot analysis for BiP expression. As shown in Fig. 3*B*, BiP protein levels were increased in cells expressing the R69H and R219S CA IV. These results indicate that the R69H and R219S CA IV mutants cause ER overload and activate the ER stress response, as previously shown for the signal sequence mutant, R14W (2).

Dominant-Negative Effects of R69H and R219S CA IV Mutants. Others previously reported that wild-type CA IV stimulated NBC1-mediated changes in intracellular pH when CA IV and NBC1 cDNAs were co-transfected into HEK-293 cells. They attributed this effect to formation of a complex between these 2 proteins to create a "functional metabolon." The CA IV mutants associated with RP17 failed to enhance NBC1 function in this assay (3, 4). We hypothesized that this impairment in NBC1 function might be due to a dominant-negative effect of the unprocessed CA IV mutants on trafficking of NBC1 from the ER to the cell surface, its functional location. To test this hypothesis, we co-transfected HEK-293 cells with NBC1 cDNA and a plasmid expressing wild-type or mutant CA IVs or vector only in a 1:1 ratio. Cell-surface expression of NBC1 was measured by cell surface biotinylation followed by immunoprecipitation with NBC1 antibody and blotting with streptavidin-HRP (Fig. 4*A*, *Upper*). Total NBC1 expression and uniform loading were

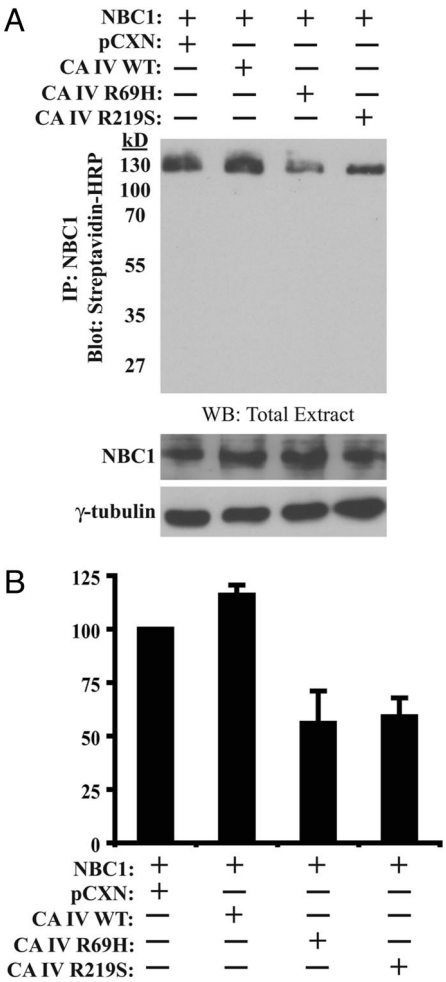

Fig. 4. Dominant-negative effects of R69H and R219S CA IV on cell-surface expression of NBC1. (*A*) HEK-293 cells were co-transfected with NBC1 and either of the indicated constructs (2.5 μg of each cDNA). Total cell surface proteins were biotinylated and the cell lysates (700 μg total protein) were subjected to immunoprecipitation (IP) with NBC1 antibody. Immunoprecipitates were analyzed on a 10% SDS/PAGE and the blots were probed with streptavidin-peroxidase (*Upper*). Parts of the lysate were also subjected to western blot (WB) with indicated antibodies (*Lower*). (*B*) Densitometry analysis of the blots to quantitate relative cell surface expression of NBC1 under each condition.

confirmed by western blot analysis on the same lysates (Fig. 4*A*, *Lower*). Co-expression of wild-type CA IV showed a slight increase in NBC1 cell-surface expression when compared with the co-transfecting vector control. However, we observed nearly a 50% reduction in cell-surface expression of NBC1 when co-expressed with either of the CA IV mutants (Fig. 4 *A* and *B*). A similar reduction was also seen with R14W CA IV (data not shown). These results support our hypothesis.

Effects of R69H and R219S CA IV Mutants on Apoptosis: Protective Role of a CA Inhibitor. Next, we asked whether ER stress produced by the processing-defective CA IV mutants can cause cell death. To answer this question, we measured the extent of apoptosis by TUNEL staining following transfection in two different cell types (COS-7 and HEK-293). The increased number of TUNEL-positive cells associated with expression of mutant CA IV indicated that both R69H and R219S induced apoptosis (Fig. 5*A*). Quantitation of all our data from both cell types showed that approximately 60% of the cells expressing either of the

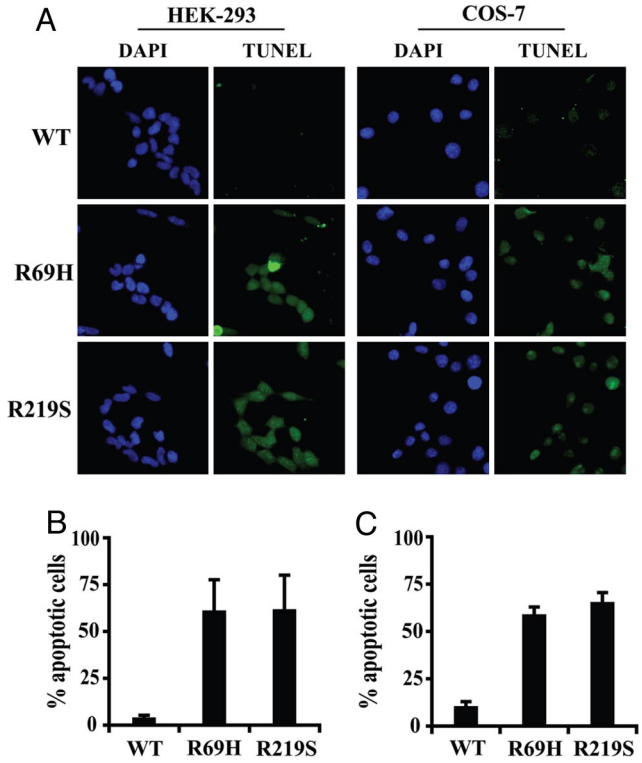

Fig. 5. Evaluation of apoptosis in cells expressing the wild-type or mutant CA IVs. (*A*) TUNEL (green) staining of HEK-293 or COS-7 cells expressing either wild-type, R69H, or R219S CA IV. Total number of cells in a field is indicated by DAPI (blue) staining. (*B*) Quantitation of TUNEL-positive HEK-293 or (*C*) COS-7 cells expressed as a percentage as a percentage of CA IV-positive cells.

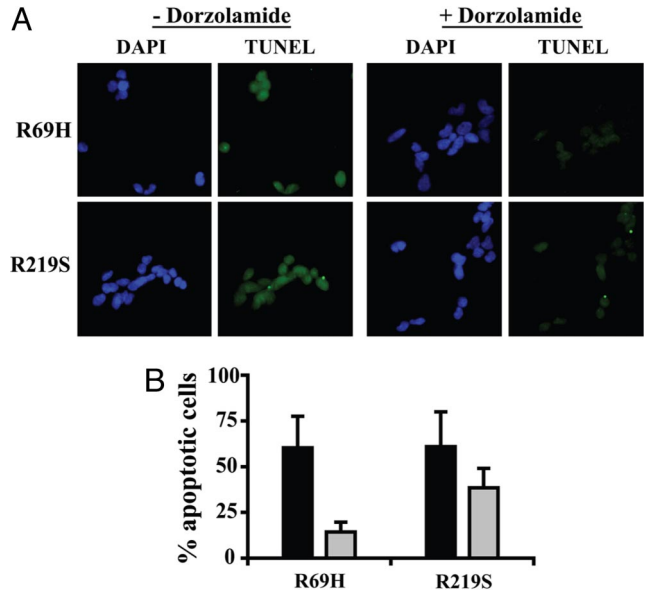

Fig. 6. Effect of dorzolamide treatment on apoptosis of HEK-293 cells expressing R69H or R219S CA IV. (*A*) TUNEL (green) staining of HEK-293 cells expressing either R69H or R219S CA IV in absence (-) or presence (+) of 10 μM dorzolamide. Total number of cells in a field is indicated by DAPI (blue) staining. (*B*) Quantitation of TUNEL positive cells treated with (gray bars) or without (black bars) dorzolamide.

mutants (R69H or R219S) were TUNEL-positive as opposed to less that 10% for the wild-type CA IV expressing cells (Fig. 5 *B* and *C*). We previously reported a similar apoptosis-inducing property for the signal sequence mutant, R14W CA IV (2). Thus, all 3 mutations associated with RP17 are capable of inducing ER stress and apoptosis.

Because CA inhibitors were shown earlier to correct the apoptosis-inducing effects of the signal sequence variant CA IV (R14W) (8), we hypothesized that CA inhibitors might also improve folding in R69H and R219S mutant proteins and protect cells from ER stress and apoptotic effects. The transfected cells were treated with 10 μM dorzolamide and studied for apoptosis by TUNEL staining (Fig. 6*A* and *B*). Apoptosis caused by the R69H mutant was reduced from 60% to 14%. Prevention of the R219S CA IV induced apoptosis by dorzolamide was less complete (from 60% to ≈40%).

Discussion

We report here that 2 RP17-associated CA IV mutations, R69H and R219S, both impaired trafficking of CA IV to the cell surface, resulting in the intracellular accumulation of misfolded proteins. Expression of both mutant CA IVs led to ER stress, had a dominant-negative effect on trafficking of other proteins that transit through the ER, and led to cell death by apoptosis. Treatment with dorzolamide, a commonly used CA inhibitor, provided protection against cell death caused by either of the mutant proteins. Our findings suggest that toxic gain of function of these CA IV mutants is the molecular basis for their retinal pathogenesis and that the use of CA inhibitors might be a promising approach to treat this disease.

Impaired processing and other properties of the R69H and R219S mutants described here are similar to those we previously characterized for the R14W variant of CA IV (2, 8). However, unlike the R14W mutation, which interferes with signal sequence processing, these mutations affect the structure of the mature protein. The Arg^{219} residue is located in the β12-strand, flanked by several hydrophobic residues (Tyr^{217}, Phe^{218}, Tyr^{220}, and Leu^{221}) (6, 10). Folding of CA II, which shares significant structural homology with CA IV, is extremely sensitive to mutations in this β-strand region (13). We suspect that the R219S mutation is a conformation-destabilizing mutation that disrupts the active site of CA IV and leads to a drastic loss of activity. Because ER quality control ensures that only correctly folded proteins leave the ER (14), most of the R219S CA IV never reaches the cell surface. The R69H mutation causes much less disruption in processing and cell-surface delivery of the mutant protein.

Mutations that impair trafficking of cell surface proteins like CA IV from the ER to the cell surface might overload the ER and cause ER stress (12). Indeed, we found that cells expressing R69H and R219S CA IV showed evidence of ER stress, the severity of which correlated with their degree of trafficking defect. We hypothesized that the ER stress would also disrupt the secretory function of ER, as reported in several other conformational diseases (15–17). Reduced cell-surface expression of NBC-1 in cells co-expressing R69H or R219S CA IV supports this hypothesis. The dominant-negative disruption in NBC1 trafficking provides an alternate explanation for the reported functional defect in NBC1-mediated HCO_3^- transport in cells co-expressing NBC1 and the CA IV mutants associated with RP17 (3, 4). This defect had previously been attributed to disruption of the NBC1-CA IV metabolon function, either due to decreased physical interaction (R14W and R69H mutations) or due to altered catalytic activity of R219S CA IV (3, 4). This loss of function theory, however, does not explain the dominant inheritance pattern of the disease or the absence of any retinal abnormality in the CA IV-knockout mouse (9).

Although the R69H mutation was less severe than R219S in disrupting trafficking of CA IV to the cell surface, both were nearly equivalent in inducing apoptosis. Thus, sustained accu-

mulation of both unfolded proteins exceeded the threshold of ER stress required to induce apoptosis. ER stress-induced apoptosis has been implicated in several human disorders, including diabetes, Parkinson's disease, Alzheimer's disease, hypoparathyroidism, and also in 1 form of RP caused by the P23H rhodopsin mutation (17–21). That ER stress may be a pathogenic mechanism underlying retinal degeneration was also suggested by Colley *et al.*, who found that NinaA, a photoreceptor specific homologue of cyclophilin, was required for export of Rh1 rhodopsin from the ER. Mutation in ninaA resulted in accumulation of Rh1 in the ER and a large buildup of rough ER membranes (22).

However, unlike rhodopsin or NinaA, CA IV is not expressed in the retina, but rather in the endothelial cells of the choroidal capillary bed (5). Hence, we propose that RP17 is primarily a disease of the choriocapillaris. The pathology in the retina is most likely secondary to the ER stress and/or apoptotic damage to the endothelial cells of the capillaries, which provide the retina its nourishment. Release of inflammatory cytokines from the ER-stressed endothelial cells of the choriocapillaris or ER stress-related oxidative stress leading to ischemic reperfusion could also contribute to this secondary retinopathy (23). Demonstration of ER stress and apoptosis induction by all 3 CA IV mutants associated with RP17 provides a unified hypothesis to explain how a single mutant allele could produce this dominant disease by a gain-of-function mechanism.

Strategies to rescue misfolded proteins in conformational diseases using chemical chaperones has recently attracted wide attention (24). An improvement in folding and processing of the R14W CA IV by several CA inhibitors has been reported (8). Here, we reported that the adverse effects of R69H and R219S CA IV mutants can also be partially abrogated by dorzolamide. We suggest that dorzolamide facilitates folding of the mutant CA IVs by binding to the active site. R219S, being an active-site mutation, markedly reduces the CA inhibitor binding affinity of CA IV. This may explain why dorzolamide treatment was less effective in rescuing the R219S mutant than the R69H. Given the proven efficacy of CA inhibitors in treating other ophthalmic diseases like glaucoma and cystoid macular edema in RP (25, 26), we suggest that CA inhibitors may provide a safe and effective approach to therapy for RP17.

One puzzling question remains to be resolved. A recent study revealed that the CA IV R14W mutation, originally identified in RP17 patients of South Africa (2), is a benign polymorphism in a population of northern Sweden (27). How could they be free of the disease if this mutation caused RP17 in South Africans? Although, genetic variability is 1 possible explanation, environmental factors could also play a crucial role in the course of disease progression. We hypothesize that Swedish individuals with the CA IV R14W mutation do not have RP17 like South African patients because they are exposed to far less sunlight. The annual average solar radiation (insolation) in Umea, Sweden and Johannesburg, South Africa are 2.7 and 5.5 kWh/m^2/day, respectively (http://eosweb.larc.nasa.gov/sse/). Exposure to light has been proven to be deleterious for photoreceptors and choroidal endothelial cells (28, 29). Thus, intense exposure to sunlight may constitute a "second hit" to the ER-stressed choricapillaris and play a determining role in retinal pathogenesis. This explanation, if true, would suggest that protection of eyes from light exposure from an early age in carriers of CA IV R14W mutation might turn the South African eye disability into the mild or nonexistent phenotype seen in Sweden.

Materials and Methods

Antibodies and Other Reagents. Anti-human NBC-1 C-terminal peptide antiserum was raised using previously described methods (30). Anti-human CA IV was described earlier (2). BiP antibody was from Santa Cruz Biotechnology. Anti-γ-tubulin, anti-rabbit IgG-peroxidase, streptavidin-peroxidase, 1,4-diazabicyclo[2.2.2]octane (DABCO), and 4′,6-diamidino-2-phenylindole (DAPI) were purchased from Sigma-Aldrich.

Construction of Mammalian Expression Vectors. Construction of human wild-type CA IV in the pCXN vector was described earlier (2). The R69H mutation was introduced using QuikChange II Site Directed mutagenesis Kit (Stratagene) and the following sense primer (with its antisense counterpart): 5′GTGGACAAAAAACTGGGACACTTCTTCTTCTCTGGCTAC3′. CA IV R219S in the pEYFP vector was a kind gift from Dr. Kang Zhang, University of Utah, Salt Lake City, UT (3) and human NBC-1 was a kind gift from Dr. George Seki and Dr. Hideomi Yamada of Tokyo University, Tokyo, Japan (31). Both cDNAs were subcloned into pCXN.

Cell Culture and Transfection. COS-7 and HEK-293 cells (American Type Culture Collection) were grown in Dulbecco's Modified Eagle's Medium (DMEM) containing 2 mM L-glutamine and 10% heat-inactivated FBS in a humidified atmosphere of 5% CO_2 at 37 °C. The transfection procedure is as described earlier (20). All experiments were performed at 72-h post-transfection. Wherever indicated, cells were incubated with 10 μM dorzolamide (Trusopt) (Merck) during the entire post-transfection period.

CA Assay. Harvested cells were resuspended in assay buffer (25 mM Tris-SO_4, pH 7.5, + 1 mM each of phenylmethylsulfonyl fluoride, orthophenanthroline, EDTA, and benzamidine chloride as protease inhibitors) and lysed by sonication. Cell lysates were measured for CA activity by the end-point titration method (32). Protein concentration of each cell lysate was determined by microLowry assay using BSA as a standard (33).

Western Blot Analysis. Harvested cells were lysed by sonication in ice cold PBS, pH 7.5, containing the protease inhibitors. Cell lysates containing 10–20 μg of total protein were analyzed by SDS/PAGE under reducing or nonreducing conditions following Laemmli's procedure (34).

Cell Surface Biotinylation Followed by Immunoprecipitation. Cells were washed with cold PBS and incubated with membrane impermeable EZ-Link Sulfo-NHS-LC-biotin (Pierce) (200 μg/mL in PBS) for 30 min at 4 °C. Excess biotin was quenched by incubating the cells with 100 mM NH_4Cl in PBS, pH 7.5, for 10 min at 4 °C after which the cells were harvested. Cells were then resuspended in lysis buffer (50 mM Tris-Cl, pH 7.5, 150 mM NaCl, 1% Triton X-100, and protease inhibitors), lysed by sonication, and clarified at 13,000 $\times$ *g* for 30 min. Protein concentration in different samples was adjusted to same values with lysis buffer. Thus, equal volumes of lysates (200–700 μg total protein) were subjected to immunoprecipitation with appropriate antibody overnight at 4 °C. The immune-complex was collected with 40 μl of 50% slurry of protein A agarose and washed 4 times with cold lysis buffer. Bound proteins were eluted by boiling in SDS/PAGE sample buffer, resolved on a 10% gel, and probed with streptavidin-peroxidase.

RNA Isolation and RT-qPCR. Total cellular RNA was prepared using RNAeasy kit (Qiagen). Resulting RNAs (2 μg/reaction) were then reverse transcribed using oligo d(T)$_{16}$ and MuLV reverse transcriptase (Applied Biosystems) and aliquots of cDNA were used as templates for RT-qPCR. Following primers were used: human BiP (forward): 5′-CGGGCAAAGATGTCAGGAAAG-3′; human BiP (reverse): 5′-TTCTGGACGGGCTTCATAGTAGAC-3′; human CHOP (forward): 5′-ACCAAGGGAGAACCAGGAAACG-3′; and human CHOP (reverse): 5′-TCACCATTCGGTCAATCAGAGC-3′. Human β-actin mRNA levels served as internal normalization standard. RT-qPCR was performed using SYBR Green JumpStart *Taq* Ready Mix (Sigma-Aldrich). Thermal cycling conditions were: 95 °C for 5 min; and 35 cycles of 95 °C/45 s, 60 °C/45 s, and 68 °C/45 s. All reactions were carried out in triplicate. The relative transcript level of the target gene was calculated as previously described (20).

Immunocytochemistry and TUNEL Staining. Immunocytochemistry was performed following previously described procedure (20). Briefly, cells were fixed with 3% paraformaldehyde and permeabilized with 0.1% Triton X-100 (for cell surface-labeling experiments, the permeabilzation step was omitted). After blocking nonspecific binding sites with 0.2% gelatin, the cells were covered with 1:500-diluted CA IV antibody followed by 1:300-diluted chicken anti-rabbit IgG-Alexafluor-546 (Molecular Probes). Slides were embedded in antiquencher solution (DABCO) containing DAPI and examined on a fluorescence microscope.

Apoptotic cells were detected using a TUNEL assay kit (Roche Applied Science) following the manufacturer's protocol. Apoptotic cells were quantified by counting the number of TUNEL-positive cells from 3 to 5 fields from at least 3 different transfections and the values were expressed as a percentage

of CA IV-positive cells (to ensure that only transfected cells are taken into account). The data are expressed as mean ± SD.

ACKNOWLEDGMENTS. The authors gratefully acknowledge Dr. Kang Zhang of the University of Utah, Salt Lake City, UT for the gift of R219S CA IV cDNA and Dr. George Seki and Dr. Hideomi Yamada of Tokyo University, Tokyo, Japan for their gift of pNBC1 cDNA. We also thank Dr. Michael Moxley and Jeffrey Grubb for helpful discussion and Tracey Baird for editorial assistance. This research was supported by National Institutes of Health grants DK40163 and GM34182 to W.S.S.

1. Hartong DT, Berson EL, Dryja TP (2006) Retinitis pigmentosa. *Lancet* 368:1795–1809.
2. Rebello G, *et al.* (2004) Apoptosis-inducing signal sequence mutation in carbonic anhydrase IV identified in patients with the RP17 form of retinitis pigmentosa. *Proc Natl Acad Sci USA* 101:6617–6622.
3. Yang Z, *et al.* (2005) Mutant carbonic anhydrase 4 impairs pH regulation and causes retinal photoreceptor degeneration. *Hum Mol Genet* 14:255–265.
4. Alvarez BV, *et al.* (2007) Identification and characterization of a novel mutation in the carbonic anhydrase IV gene that causes retinitis pigmentosa. *Invest Ophthalmol Vis Sci* 48:3459–3468.
5. Hageman GS, Zhu XL, Waheed A, Sly WS (1991) Localization of carbonic anhydrase IV in a specific capillary bed of the human eye. *Proc Natl Acad Sci USA* 88:2716–2720.
6. Okuyama T, Sato S, Zhu XL, Waheed A, Sly WS (1992) Human carbonic anhydrase IV: cDNA cloning, sequence comparison, and expression in COS cell membranes. *Proc Natl Acad Sci USA* 89:1315–1319.
7. Okuyama T, Waheed A, Kusumoto W, Zhu XL, Sly WS (1995) Carbonic anhydrase IV: Role of removal of C-terminal domain in glycosylphosphatidylinositol anchoring and realization of enzyme activity. *Arch Biochem Biophys* 320:315–322.
8. Bonapace G, Waheed A, Shah GN, Sly WS (2004) Chemical chaperones protect from effects of apoptosis-inducing mutation in carbonic anhydrase IV identified in retinitis pigmentosa 17. *Proc Natl Acad Sci USA* 101:12300–12305.
9. Ogilvie JM, *et al.* (2007) Carbonic anhydrase XIV deficiency produces a functional defect in the retinal light response. *Proc Natl Acad Sci USA* 104:8514–8519.
10. Stams T, *et al.* (1996) Crystal structure of the secretory form of membrane-associated human carbonic anhydrase IV at 2.8-A resolution. *Proc Natl Acad Sci USA* 93:13589–13594.
11. Waheed A, Zhu XL, Sly WS (1992) Membrane-associated carbonic anhydrase from rat lung: Purification, characterization, tissue distribution, and comparison with carbonic anhydrase IVs of other mammals. *J Biol Chem* 267:3308–3311.
12. Wu J, Kaufman RJ (2006) From acute ER stress to physiological roles of the Unfolded Protein Response. *Cell Death Differ* 13:374–384.
13. Krebs JF, Fierke CA (1993) Determinants of catalytic activity and stability of carbonic anhydrase II as revealed by random mutagenesis. *J Biol Chem* 268:948–954.
14. Sitia R, Braakman I (2003) Quality control in the endoplasmic reticulum protein factory. *Nature* 426:891–894.
15. Izumi T, *et al.* (2003) Dominant negative pathogenesis by mutant proinsulin in the Akita diabetic mouse. *Diabetes* 52:409–416.
16. Cooper AA, *et al.* (2006) Alpha-synuclein blocks ER-Golgi traffic and Rab1 rescues neuron loss in Parkinson's models. *Science* 313:324–328.
17. Ryu EJ, *et al.* (2002) Endoplasmic reticulum stress and the unfolded protein response in cellular models of Parkinson's disease. *J Neurosci* 22:10690–10698.
18. Ozcan U, *et al.* (2004) Endoplasmic reticulum stress links obesity, insulin action, and type 2 diabetes. *Science* 306:457–461.
19. Mattson MP, Gary DS, Chan SL, Duan W (2001) Perturbed endoplasmic reticulum function, synaptic apoptosis and the pathogenesis of Alzheimer's disease. *Biochem Soc Symp*151–162.
20. Datta R, Waheed A, Shah GN, Sly WS (2007) Signal sequence mutation in autosomal dominant form of hypoparathyroidism induces apoptosis that is corrected by a chemical chaperone. *Proc Natl Acad Sci USA* 104:19989–19994.
21. Galy A, Roux MJ, Sahel JA, Leveillard T, Giangrande A (2005) Rhodopsin maturation defects induce photoreceptor death by apoptosis: a fly model for RhodopsinPro23His human retinitis pigmentosa. *Hum Mol Genet* 14:2547–2557.
22. Colley NJ, Baker EK, Stamnes MA, Zuker CS (1991) The cyclophilin homolog ninaA is required in the secretory pathway. *Cell* 67:255–263.
23. Zhang K, Kaufman RJ (2008) From endoplasmic-reticulum stress to the inflammatory response. *Nature* 454:455–462.
24. Ulloa-Aguirre A, Janovick JA, Brothers SP, Conn PM (2004) Pharmacologic rescue of conformationally-defective proteins: implications for the treatment of human disease. *Traffic* 5:821–837.
25. Mincione F, Scozzafava A, Supuran CT (2008) The development of topically acting carbonic anhydrase inhibitors as antiglaucoma agents. *Curr Pharm Des* 14:649–654.
26. Grover S, Apushkin MA, Fishman GA (2006) Topical dorzolamide for the treatment of cystoid macular edema in patients with retinitis pigmentosa. *Am J Ophthalmol* 141:850–858.
27. Kohn L, *et al.* (2008) Carrier of R14W in carbonic anhydrase IV presents Bothnia dystrophy phenotype caused by two allelic mutations in RLBP1. *Invest Ophthalmol Vis Sci* 49:3172–3177.
28. Fain GL (2006) Why photoreceptors die (and why they don't). *Bioessays* 28:344–354.
29. Wu T, Handa JT, Gottsch JD (2005) Light-induced oxidative stress in choroidal endothelial cells in mice. *Invest Ophthalmol Vis Sci* 46:1117–1123.
30. Parkkila S, *et al.* (1997) Immunohistochemistry of HLA-H, the protein defective in patients with hereditary hemochromatosis, reveals unique pattern of expression in gastrointestinal tract. *Proc Natl Acad Sci USA* 94:2534–2539.
31. Horita S, *et al.* (2005) Functional analysis of NBC1 mutants associated with proximal renal tubular acidosis and ocular abnormalities. *J Am Soc Nephrol* 16:2270–2278.
32. Maren TH (1960) A simplified micromethod for the determination of carbonic anhydrase and its inhibitors. *J Pharmacol Exp Ther* 130:26–29.
33. Peterson GL (1979) Review of the Folin phenol protein quantitation method of Lowry, Rosebrough, Farr and Randall. *Anal Biochem* 100:201–220.
34. Laemmli UK (1970) Cleavage of structural proteins during the assembly of the head of bacteriophage T4. *Nature* 227:680–685.